A Comprehensive Numerical Approach to the Modeling and Simulation of Plume Interaction Effects on Solar Electric Propulsion Spacecraft

IEPC-2017-238

Presented at the 35th International Electric Propulsion Conference
Georgia Institute of Technology – Atlanta, Georgia – USA
October 8–12, 2017

Luis M. Bermúdez,* Kevin J. Barnhart,† Christine A. Agathon-Burton,‡ Debasis Basak§
and Michael J. Glogowski¶
Space Systems Group, Orbital ATK, Inc., Dulles, VA 20166-6874, USA

The widespread adoption of ion Electric Propulsion (EP) systems at Orbital ATK has necessitated the development of a comprehensive tool set for the Modeling and Simulation (M&S) of plasma plume interactions with the various spacecraft systems. These interactions can lead to physical effects, such as erosion and contamination of sensitive spacecraft surfaces; thermal-mechanical effects, such as force cross-coupling, induced torques and heating; electrical effects, such as parasitic currents and electrostatic discharge (ESD); and electromagnetic effects, such as radio-frequency (RF) signal attenuation and modulation. All of these effects must be accounted for by the spacecraft design engineer when developing an EP-enabled spacecraft compatible with the environment produced by ion electric propulsion systems. M&S capabilities have been developed at Orbital ATK for this purpose over the last four years. A toolset based on AFRL's COLISEUM software suite, Leidos' NASCAP-2k, and University of Texas' BeamServer II has been assembled and augmented with new models and post-processing techniques. Furthermore, a series of ground tests were completed at The Aerospace Corporation to provide the core materials database for the physical effects and the end-to-end test results for evaluation of the modeling predictions. These tools are now being deployed across multiple Orbital ATK spacecraft product lines, including the commercial GEOStar spacecraft, the Mission Extension Vehicle (MEV), national security missions, and human space missions. While the emphasis has been on EP systems that utilize Hall Effect Thrusters (HETs), the tool suite has been extended for use with other thrusters, such as the NASA Evolutionary Xenon Thruster (NEXT) and colloidal thrusters. This paper provides an overview of the M&S tools and capability at Orbital ATK, an example of the results produced by these tools, and a discussion on future developments.

Nomenclature

C_0	New sputter model constant, atoms/(ion$\sqrt{\text{eV}}$)
$C_{1,2,3}$	New sputter model polynomial coefficients
$C_{4,5,6}$	New sputter model polynomial exponents
E	Ion energy, eV
E_{th}	Threshold energy, eV
g	Ion incidence angle dependence function
S	Ion energy dependence function, atoms/ion
Y	Total sputter yield, atoms/ion
β	Ion incidence angle, rad

*Staff Systems Engr., Systems Engineering Dept.
†Systems Engr., Systems Engineering Dept.
‡Senior Principal Engr., Systems Engineering Dept.
§Staff Material Sciences Engr., Safety & Mission Assurance Dept.
¶Senior Director, Advanced Technology Development, Commercial Satellites.

I. Introduction

The last decade has seen an increase in the activities directed at the understanding and modeling of the flow physics generated in EP devices. The surge in interest has been mainly motivated by the adoption of EP thrusters as a technically viable and more mass efficient solution for spacecraft propulsion and by the need to understand the spacecraft interaction with the plume generated by these devices. On one side, NASA, DoD, and other research organizations have been at the forefront of the R&D effort conducting first-of-a-kind tests to uncover new physics, formulating mathematical models that allow further understanding, and advancing the simulation techniques which together have provided higher fidelity and more capable tools for the study and characterization of EP thruster flows and plumes. On the other side, industry leaders such as Orbital ATK have adopted these tools in analytical processes, augmenting existing capabilities in some instances, and contributing to the EP technology maturation roadmap.

Since 2013 the Space Systems Group of Orbital ATK has been working towards the technology infusion of EP in all aspects of the engineering design, manufacturing processes and mission operations of its Commercial, Science & Environmental, National Security, and Human Space & Advanced Systems spacecraft product lines. To this end, the GEOStar bus offers now the replacement of heritage Improved Electrothermal Hydrazine Thrusters (ImpEHTs) by the XR-5 HETs. The Mission Extension Vehicle (MEV) which will provide cooperative in-orbit satellite life extension and maneuvering services to geosynchronous satellite operators will also incorporate HETs for orbit raising, station keeping, and inclination reduction. In addition to these, several other spacecraft currently in the proposal and design stages will incorporate different types of EP solutions, including NEXT and others.

Within this frame, the Space Systems Group of Orbital ATK has been carrying out numerical M&S activities in order to evaluate the range of spacecraft-plume interaction effects. These effects which can be grouped by their nature as physical, thermal-mechanical, electrical, and RF interference are being characterized by means of tools like COLISEUM, HPHall, NASCAP-2k, and BeamServer II.

Starting with the physical effects group, AFRL's COLISEUM software suite has been used in conjunction with MIT's HPHall and other engineering particle injection models to simulate the sputtering phenomenon and quantify the erosion and contamination effects on the spacecraft structures and components. Surface erosion can be the source of mechanical weakening and modification of thermo-optical properties which can cause degradation of subsystems on-board the spacecraft. On the spacecraft, solar arrays (SA), cameras and other optical sensors are the most critical parts subject to this effect. The computation of surface erosion is mostly based on a database of sputter yields built through a series of experimental campaigns for the different materials used on the spacecraft surfaces. Like erosion, contamination results in the modification of the thermo-optical properties. Changes on absorptance, emittance, and transmittance with the deposition of sputtered materials are also characterized and included on a database for use during the post-processing stage of the COLISEUM results.

The mechanical effects come in the form of induced forces and moments on the spacecraft caused by the direct impingement of the thruster plume on the spacecraft surfaces. The magnitude of these disturbances are estimated by integrating the momentum fluxes reported by COLISEUM at the spacecraft surfaces and are used in the control system design, mission propellant budget, etc. Thermal effects caused by the same phenomenon are similarly estimated by integrating the energy fluxes reported by COLISEUM.

Electrical effects of interest include spacecraft charging and leakage current between the HET and the spacecraft ground. Charging of a spacecraft creates an electric field that can cause ESD events and affect the environment surrounding the spacecraft (i.e. enhancing erosion and contamination). A different floating potential is established by current balance between the ions incident on conductive surfaces of the spacecraft and electrons collected by biased interconnects and termination tabs on the SA cells. To determine the surface potentials, Leidos' NASCAP-2k software is used but with the plume model imported from COLISEUM rather than the PlumeTool module. Furthermore, the use of the ObjectToolkit in NASCAP-2k was replaced by a combination of Python scripts and a third-party grid generation software used for the generation of the surface meshes in COLISEUM streamlining in that way the entire numerical analysis process.

Finally with respect to the RF effects group, the concern is with HETs producing an unsteady plasma medium in the vicinity of an antenna subsystem that can cause RF interference and degrade the signal quality. Such degradation effects include pointing error and attenuation of the main antenna lobe, side lobe changes, and induced cross polarization. To characterize these effects, the University of Texas code BeamServer II is being included in the analysis toolbox.

II. Modeling & Simulation

II.A. Physical Effects

The erosion and contamination effects on the spacecraft systems are analyzed using AFRL's COLISEUM software suite. COLISEUM is a 3D framework for modeling plasma dynamics and surface interactions consisting of a set of library functions that read and execute script files, manage boundary conditions and plasma interactions, and act as a driver for a number of internal codes responsible for the plasma propagation through the computational domain. Several input files with the problem specifics must be set up during the model generation and ahead of the simulation execution.

The COLISEUM software suite models the different physical mechanisms associated with HET plasma plumes and implements a variety of total and differential sputter models to assist in the evaluation of the physical and mechanical effects of plasma plumes like erosion, sputtering, contamination, and induced forces and moments. Table 1 lists the spacecraft materials, and the sputtering and sampling (i.e. redeposition) models used in COLISEUM for addressing the erosion and contamination effects on the spacecraft.

Table 1. Spacecraft materials and the corresponding sputter and sampling models used in the erosion and contamination analysis. The source of the total sputter yield coefficients is included between parentheses. Formulation of the Yamamura, Roussel, and Modified Zhang total and differential sputter models are included in Refs. 1-2, 3 and 4, respectively.

Spacecraft Material	Sputter Model	Sampling Model
Anodized Aluminum	Yamamura-Polynomial (GA)	Cosine
Astroquartz	Yamamura-Polynomial (GA)	Cosine
Black Kapton MLI	Hofer-Bermudez (GA)	Cosine
Hexagonal Boron Nitride (h-BN)	Yamamura (Ref. 5)	Cosine
CMG Coverglass	Hofer-Bermudez (GA)	Cosine
Ge-Coated Kapton Sunshield	Hofer-Bermudez (GA)	Cosine
Graphite Fiber Reinforced Polymer (GFRP)	Hofer-Bermudez (GA)	Modified Zhang
Antireflective Coating	Hofer-Bermudez (GA)	Modified Zhang
Optical Solar Reflectors (OSR) Ultraviolet Radiation Layer	Yamamura-Polynomial (GA)	Cosine
Room-Temperature Vulcanizing (RTV) Silicone	Yamamura (GA)	Cosine
Indium Tin Oxide (ITO) Coated Glass	Roussel (Ref. 6)	Cosine
Kapton	Roussel (Ref. 6)	Cosine
Teflon	Roussel (Ref. 6)	Cosine

Orbital ATK planned and conducted a test campaign with some of the tests aimed particularly at collecting the necessary data for direct determination of the total sputter yield of spacecraft materials.[7] It was also designed to determine the change in thermo-optical properties due to erosion. The technique consisted of exposing representative sample materials to an ion plume from a calibrated ion source under controlled conditions for a predetermined length of time and measuring the mass loss due to the resultant erosion. Sputter yield was then calculated for a given ion energy and incident angle by measuring mass loss, current density, and test duration. These tests were conducted in a large vacuum chamber with a number of test instruments hard-wired to it. The tests were conducted over a range of energies and incident angles with measurements made at five discrete incident angles for each energy level.

A parallel effort to the total sputter yield tests was undertaken to develop a Genetic Algorithm (GA) which provides the total sputter coefficients that best fit the experimental data collected.[8] Those spacecraft materials where the total sputter model coefficients were determined following this approach are identified in table 1.

In the process of finding the total sputter model coefficients, it was determined that none of the models included in COLISEUM provided a good fit for some of the spacecraft materials characterized. Therefore a new sputter model was formulated following the functional structure given in

$$Y\left(E,\beta\right) = S\left(E\right) g\left(\beta\right) \tag{1}$$

with the ion energy dependence relation given by Hofer *et al.*[9]

$$S\left(E\right) = C_0\sqrt{E}\left(1-\sqrt{\frac{E_{th}}{E}}\right)^{2.5} \tag{2}$$

and the following four-term polynomial of argument β for the ion incidence function

$$g(\beta) = 1 + C_1 \beta^{C_4} + C_2 \beta^{C_5} + C_3 \beta^{C_6} \quad (3)$$

where

$$C_3 = -C_1 (\pi/2)^{C_4 - C_6} - C_2 (\pi/2)^{C_5 - C_6} - (\pi/2)^{-C6} \quad (4)$$

in order to fulfill the condition $g(\pi/2) = 0$.

The new model is listed as *Hofer-Bermudez* in table 1 and depicted in Fig. 1 for the MgF_2 antireflective coating.[8] Finally with respect to the sputter computation, the coefficients for the Yamamura total sputter model provided in Refs. 1 and 2 are used for those spacecraft materials made of pure elements.

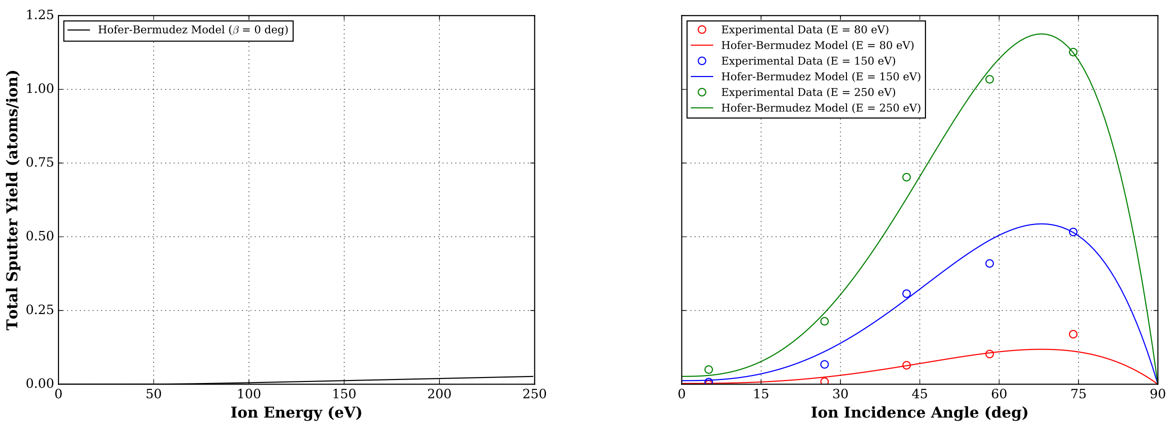

Figure 1. MgF_2 total sputter yield experimental data and model.

COLISEUM incorporates several options to set the required boundary condition (BC) representing the thruster particle injection into the simulation. Others have been developed at Orbital ATK and added to the COLISEUM source database. The most common particle injection models used in the M&S of the plasma plume physical interaction effects on spacecrafts are described next.

II.A.1. Aerojet Rocketdyne XR-5 HET

Among the particle injection models for Aerojet Rocketdyne XR-5 HET are the Retarding Potential Analyzer (RPA) and the HPHall sources:

- The RPA source uses a series of RPA readings to define the number and energy of the injected ions. In essence, this source is a statistical representation of a ray tracing. As such, it does not allow for background pressure corrections but offers faster execution time.
- The HPHall code was originally developed by Fife and Martínez-Sánchez,[10] upgraded to HPHall-2 by Parra and Ahedo[11] and subsequently improved by the Electric Propulsion group at NASA Jet Propulsion Laboratory (JPL).[12] An Orbital ATK customized version of HPHall also incorporates the updates introduced by Smith[5] relative to the addition of triply-charged xenon ions, and the erosion submodel.

In the case of HPHall, a calibration procedure is required in order to find the model coefficients representing the anomalous electron mobility that results in better correlation with the plume properties experimental data. To this end, Langmuir and RPA probe data collected at one meter distance was used. Comparisons between the experimental data and the simulation results are depicted in Fig. 2.

In addition to the sputter yield material characterization tests, another test in the campaign was planned and conducted to evaluate the impact of the XR-5 HET plume on the spacecraft surfaces. This test, referred as the *end-to-end verification test*, aimed to determine the rate and amount of erosion and contamination on two relevant spacecraft materials due to plume impingement. Those materials were the antireflective (MgF_2) coated CMG cover glass and the M55J/954-3 graphite fiber reinforced polymer (GFRP).[8]

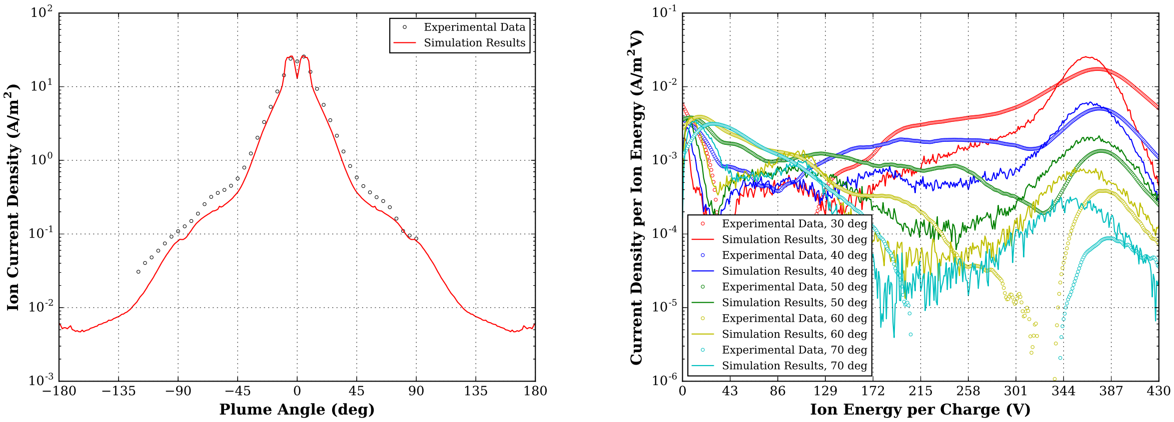

Figure 2. Langmuir (left) and RPA (right) probe data @ 1 m for the XR-5 HET @ 400 V & 3 kW operating condition.

The mass loss and deposition measured on the erosion and contamination samples during the end-to-end verification test were then used to determine the degree of accuracy of the simulation process in general, and the sputter modeling and thruster calibration in particular. For that purpose, the test configuration set up shown in Fig. 3 was modeled and the simulation executed using the sputter correlations and thruster calibration described previously. The results are shown in tables 2, 3, 4 and 5.

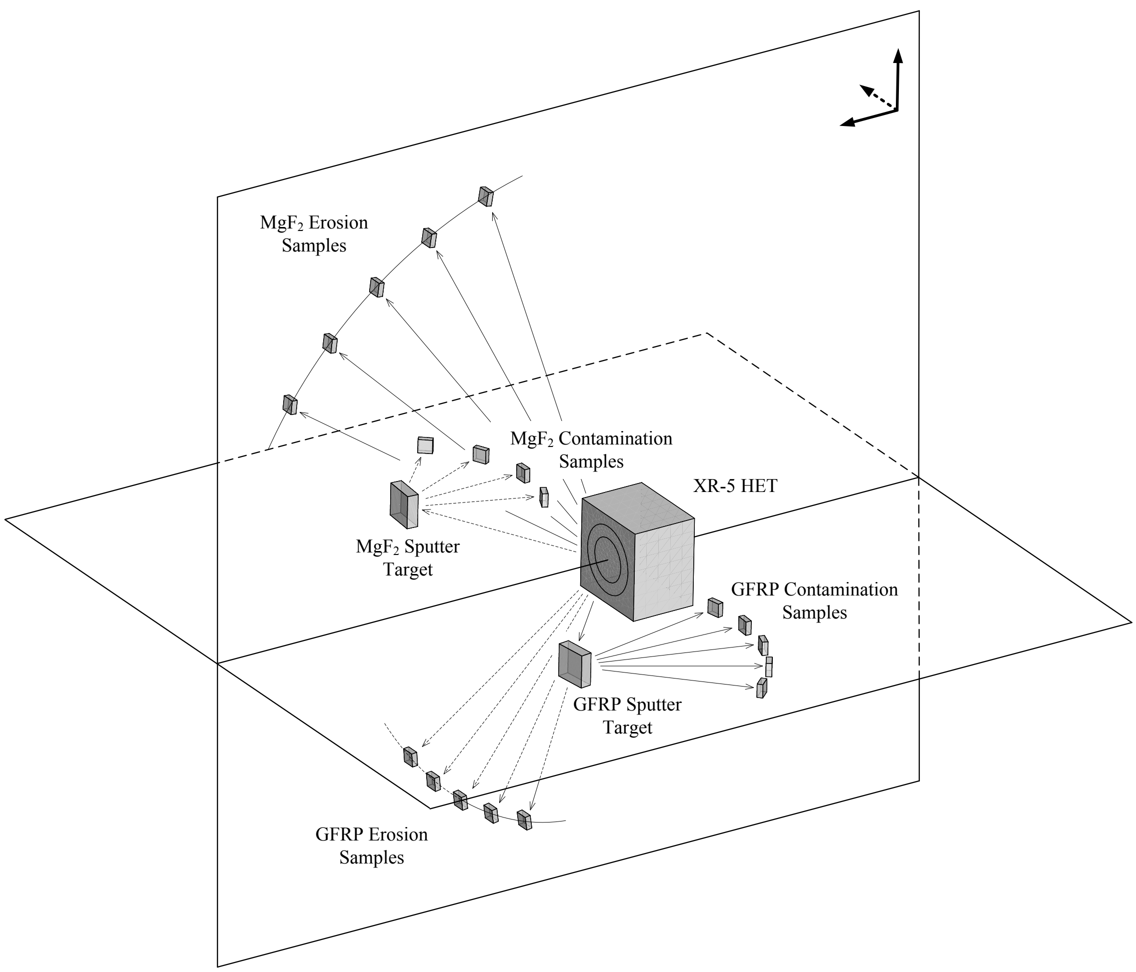

Figure 3. End-to-end verification test set up.

Table 2. MgF_2 erosion during the end-to-end verification test.

Plume Angle (deg)	Incidence Angle (deg)	Experimental Data ($\mu g/cm^2$)	Simulation Results (RPA Source) ($\mu g/cm^2$)	Simulation Results (HPHall Source) ($\mu g/cm^2$)
71	62	-4.1	-5.7	-12.0
62	54	-12.0	-13.9	-30.3
53	46	-18.1	-12.1	-18.8
44	38	-53.5	-28.0	-25.6
35	30	-146.8	-54.6	-41.8

Table 3. GFRP erosion during the end-to-end verification test.

Plume Angle (deg)	Incidence Angle (deg)	Experimental Data ($\mu g/cm^2$)	Simulation Results (RPA Source) ($\mu g/cm^2$)	Simulation Results (HPHall Source) ($\mu g/cm^2$)
71	62	-12.3	-4.5	-21.9
62	54	-25.0	-17.9	-62.7
53	46	-56.9	-64.5	-131.1
44	38	-150.9	-210.6	-239.0
35	30	-427.2	-618.2	-582.8

Table 4. MgF_2 contamination during the end-to-end verification test.

Angle with respect to Target Normal (deg)	Experimental Data (μg)	Simulation Results (RPA Source) (μg)	Simulation Results (HPHall Source) (μg)
-37.5	3.7	3.4	7.9
-12.5	12.0	3.6	11.0
12.5	15.6	5.0	11.0
37.5	13.1	4.5	13.2

Table 5. GFRP contamination during the end-to-end verification test.

Angle with respect to Target Normal (deg)	Experimental Data (μg)	Simulation Results (RPA Source) (μg)	Simulation Results (HPHall Source) (μg)
-19	4.7	5.5	10.3
0	8.3	4.9	8.1
19	19.0	4.4	8.9
37	15.8	3.6	10.9
54	21.0	4.7	9.5

Concerning the MgF_2 erosion part of the end-to-end verification test, hand calculations performed using raw plume and sputter yield data in addition to the simulation results included in table 2 point to the fact that the MgF_2 total sputter yield at small incidence angles is underestimated by the sputter model. This is confirmed after looking at the comparison between the model predictions and the experimental data shown in Fig. 1.

Furthermore, although a second test carried out to characterize the XR-5 plume resulted in significant variability of the plume energy content distribution, Fig. 2 also shows that the HPHall source model underestimates the ion population at medium to low energy levels (i.e. elastic scattered and CEX ions) while it overestimates it at high energy levels (i.e. primary ions). This latter observation is especially true at high plume angles and is the reason for the prediction of high levels of erosion of the MgF_2 in the end-to-end verification test.

Similar hand calculations to those mentioned earlier and the simulation results for GFRP erosion shown in table 3 demonstrate the suitability of the total sputter yield model generated for this material. The simulation results using the HPHall source in this particular case suffer from the same model deficiencies as described before.

Finally with respect to the contamination simulation results shown in tables 4 and 5, all use the Modified Zhang sampling model in COLISEUM. The sputter targets for both materials (see Fig. 3) were situated at plume incidence angles where the total sputter yield approximate maximum values. In this case and at these particular plume and incidence angles, the HPHall source model provides closer results to the experimental data than the RPA source model. This part of the end-to-end verification test carries many challenges in the test data reduction and numerical simulation; its main usefulness is to serve for establishing uncertainties on the contamination numerical predictions.

The ultimate objective of the M&S effort in the area of physical effects is the ability to estimate the erosion and contamination levels on all the spacecraft surfaces due to the HET plume impingement at any thruster operating condition during any of the spacecraft orbit phases. This is shown in Figs. 4 and 5 for the contamination from all the spacecraft sputtered materials on the MEV during station-keeping and for the erosion on the antireflective coating on a non-GEO satellite after a full rotation of the SA, respectively. Furthermore, erosion and contamination effects on the spacecraft optical sensors (i.e. star trackers, sun sensors, cameras, etc.) are of particular interest due to their potential for degradation of the thermo-optical properties. This is clearly depicted in Fig. 6 where the effect of germanium and carbon thin film contamination on magnesium fluoride (MgF_2) coated CMG cover glass is estimated using a thin-film optical simulator.

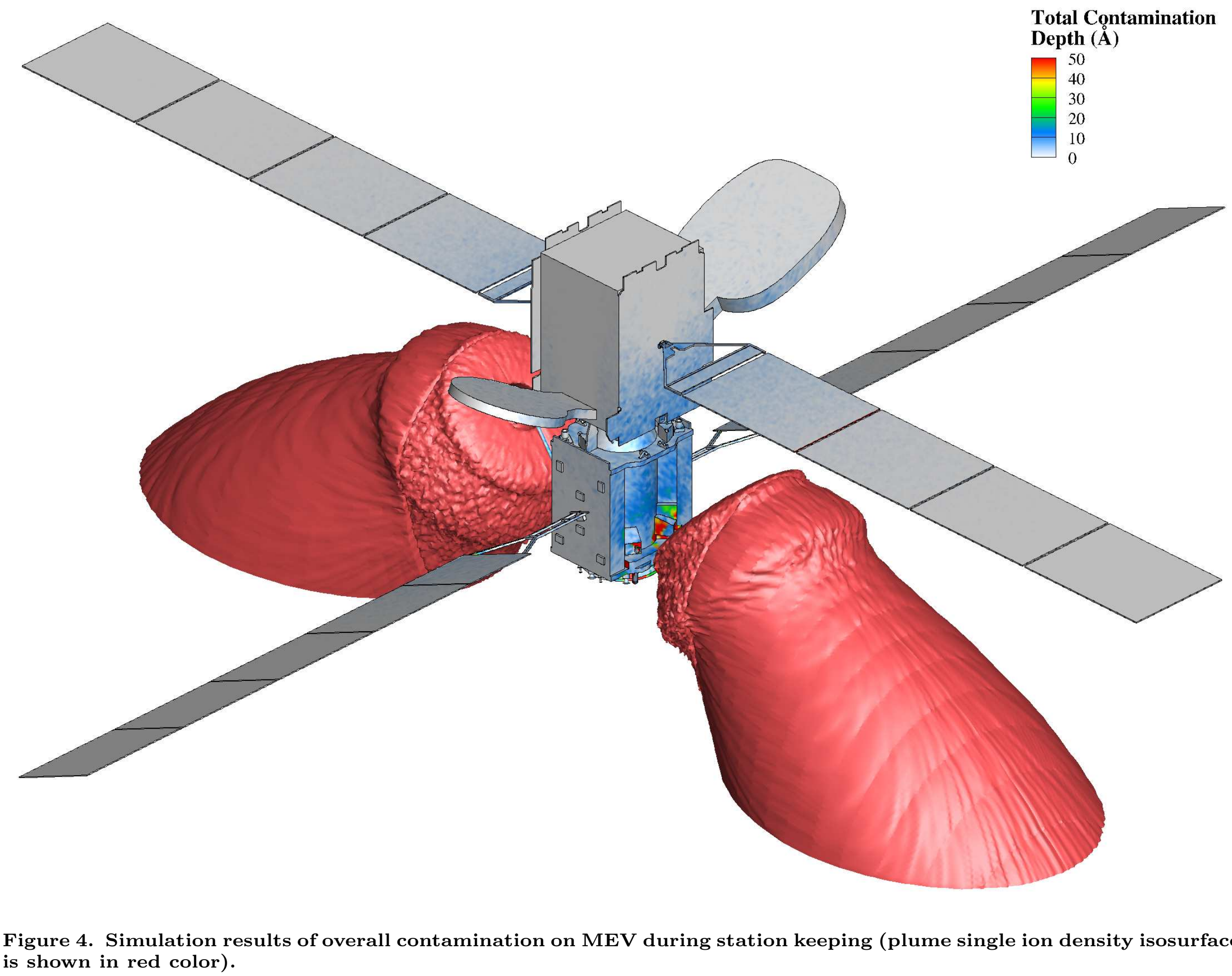

Figure 4. Simulation results of overall contamination on MEV during station keeping (plume single ion density isosurface is shown in red color).

In this particular area a series of contamination tests and thermo-optical properties measurements were also planned and conducted on a set of critical spacecraft materials. A single test consisted of one sputter target and four composite contamination targets. Gold sample-sets were also exposed under identical conditions, as standard samples. Each sputter target was placed at a fixed distance (nominally 7 in) from the ion source. The ion beam passed through a beam aperture and illuminated the target at a fixed incident angle

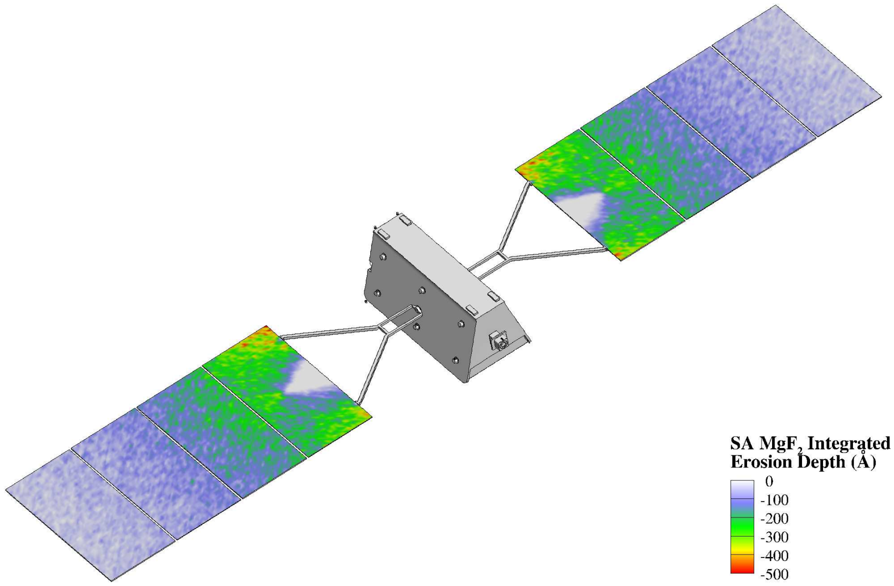

Figure 5. Simulation results of erosion on the SA MgF_2 coating of a non-GEO satellite SA after a full rotation.

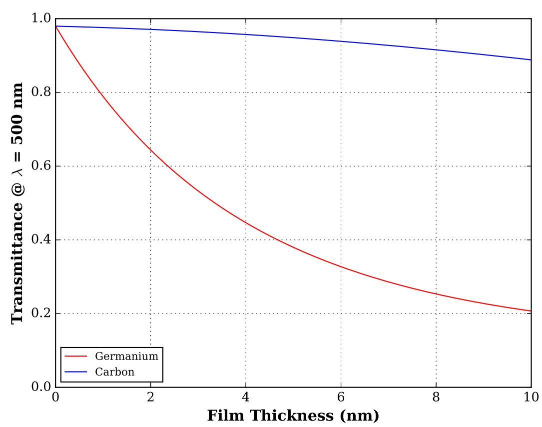

Figure 6. Transmittance change on the MgF_2 coated glass due to thin film contamination of Ge and C.

of 60 deg. Sputtered ejecta was then deposited on the contamination sample-set which was behind a grafoil mask. The target to sample distance was nominally 3 in. Contamination samples were all 1-inch square and were mounted in a specially designed quadrant sample holder. Once the measured delta mass before and after exposure was determined, it was converted to an estimated thickness change using contaminant flux, material density, and area exposed. Other approximations were also applied, such as, deposition rate based on a fixed time stamp, azimuthal flux ratio, and sticking coefficient.

In addition to this, erosion and contamination samples underwent pre- and post-exposure thermo-optical measurements to determine the change due to the ion beam exposure. For erosion tests, spectral transmittance was measured for antireflective coating and CMG coverglass. Solar absorptance was measured for Black Kapton and Ge-coated Kapton. For contamination tests, solar absorptance and IR emittance was measured on Black Kapton, Ge-coated Kapton, anodized aluminum, and OSR. The measurements were done with the following materials as targets: antireflective coating, CMG coverglass, GFRP, RTV, and Black Kapton. An example of the the simulation results for the loss of solar absorptance due to the antireflective coating contamination is shown in Fig. 7 for the GEOStar spacecraft.

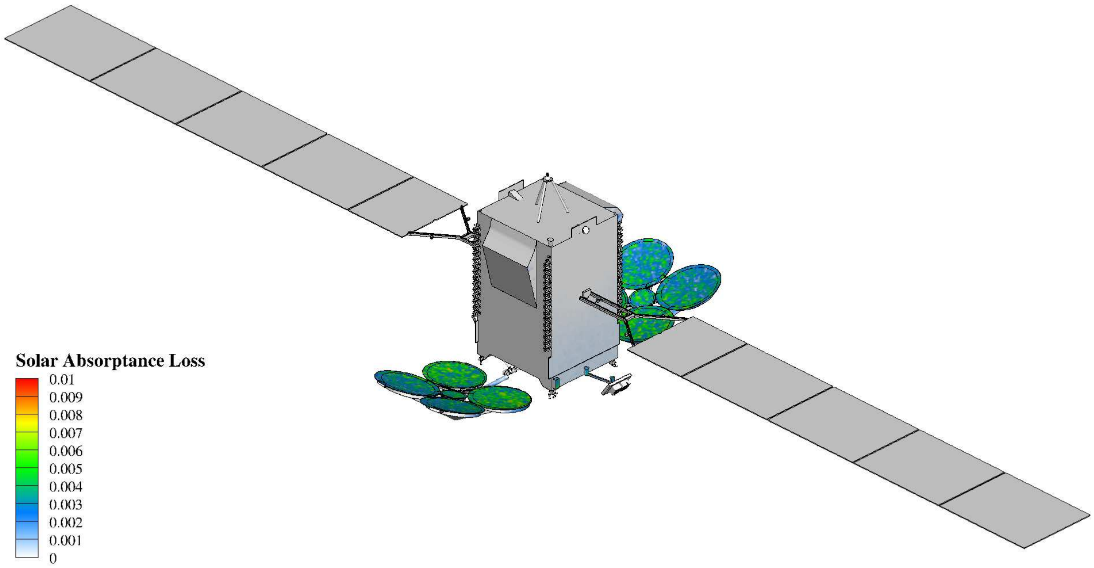

Figure 7. Simulation results for the loss of solar absorptance due to MgF_2 contamination for the GEOStar spacecraft.

II.A.2. NASA Evolutionary Xenon Thruster (NEXT)

The potential for contamination on critical spacecraft surfaces of the material eroded from the NEXT during operation has been the main motivation behind the M&S work carried out at Orbital ATK on this particular EP thruster. The deposition of the molybdenum particle flux emanating from the NEXT extraction grids and the subsequent generation of molybdenum ions by CEX between the sputtered material and the Xenon ions can negatively affect the thermo-optical properties of the spacecraft surfaces. The aforementioned M&S effort encompassed the validation of the NEXT particle injection model included within the COLISEUM framework (see Ref. 13) and the incorporation of a kinetic description of the Mo injection for all thrust levels (TLs) in the throttle table (i.e. TT11) developed for planetary science missions. A companion paper by Bermúdez and Jermakian describes in detail the steps taken during the generation and validation of this model.

In particular, the most relevant step in the validation process involved comparing grid material deposition rates between the simulation results and the experimental measurements performed on a rotatable quartz crystal microbalance (QCM) as presented in Ref. 14. Figure 8 shows the test set up used for the QCM measurements and the simulated Mo plume ejected from the NEXT acceleration grid while Fig. 9 depicts the net mass deposition for a representative thrust level. The agreement between the experimental data and simulation results is good for high plume angles where the CEX ion population is predominant. However, the comparison worsens near the beam centerline where the more energetic ions reside and the plume structure suffers the most based on the simulation approach taken in this analysis.

II.A.3. Accion Systems TILE Ion Electrospray Thruster

Another effort is currently underway at Orbital ATK to develop a source model of Accion Systems TILE ion electrospray thruster for the COLISEUM framework. The model primarily builds on the works of Paulo Lozano and Manuel Gamero-Castaño (see Refs. 15 and 16) and incorporates novel approaches to model the electrospray thruster as a general problem. The generality of the problem stems primarily from the complexity of the plume structure and a dearth of experimental diagnostics. For instance, in the ion-droplet mixed operating regime a number of distinct ion species and a near infinite number of droplet species are generated over a large spectrum of charge to mass ratios. The fundamental challenge is to determine the composite species of the plume while incorporating the particle-particle interactions that are essential to the resulting plume.

Figure 10 shows the implementation of the source model for the anticipated Accion Systems TILE thruster

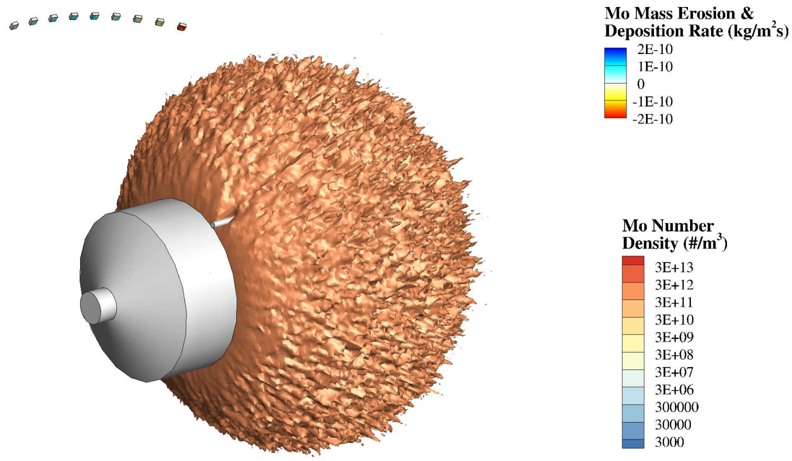

Figure 8. QCM test setup.

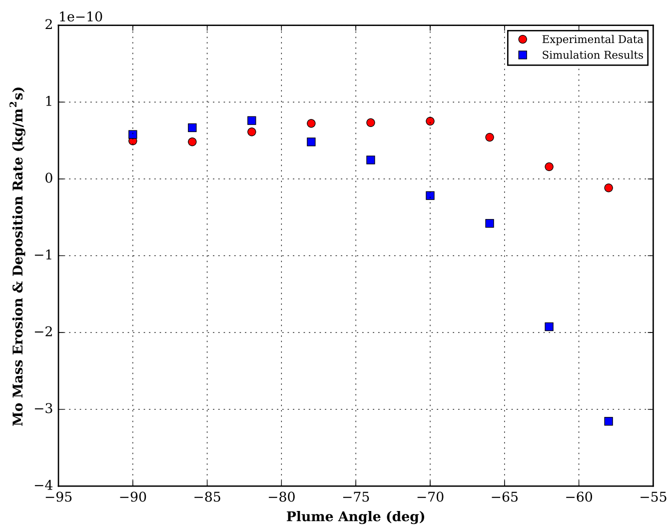

Figure 9. Net mass deposition rate for TL37.

chip, the fundamental component of the TILE thruster, in the ion-droplet mixed regime. In this case strict restraints are imposed, namely, a uniform monoenergetic beam. The model is presently undergoing revisions to incorporate arbitrary energy distributions and increase the fidelity of the plume's angular composition. A validation campaign has also been partially completed at this point.

II.B. Thermal-Mechanical Effects

Mechanical effects induced by the plasma plume impingement are important for evaluating the robustness of the control system and assessing the propellant budget during different parts of the mission where electric propulsion is used. Thermal effects induced by the same phenomenon are also accounted for in the thermal design spacecraft. Figures 11 and 12 show a typical history of the dynamics and energy induced on the spacecraft for a full rotation of the SA.

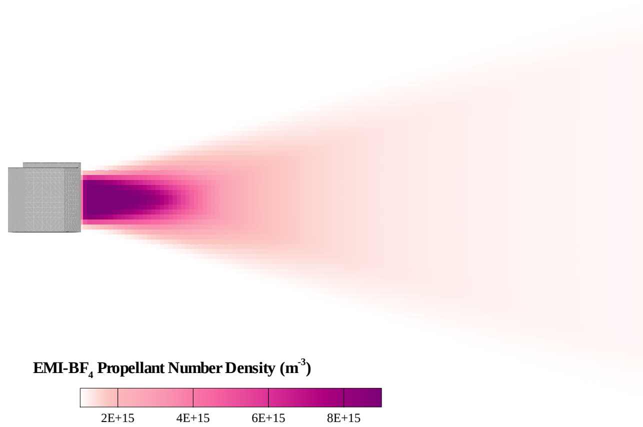

Figure 10. Electrospray source model representation of the TILE chip. Three ion and five droplet species are injected from a specified array of 1920 individual emitters. Operating conditions are taken from Ref. 17.

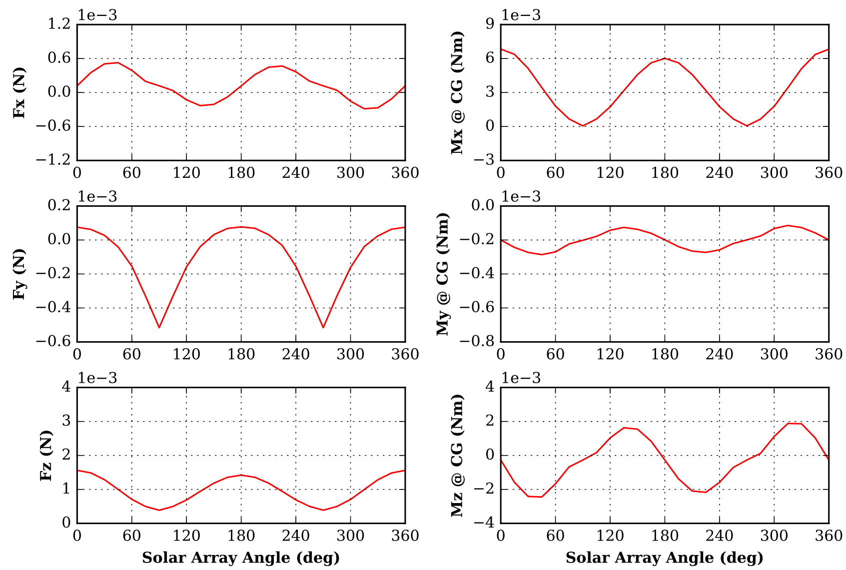

Figure 11. Induced forces and moments on the spacecraft due to plume impingement from the XR5 HET.

II.C. Electrical Effects

With respect to electrical interaction effects caused by the thruster plume impingement, charging and leakage current between the HET and the spacecraft ground are of particular concern. Spacecraft surface potentials produced through plasma plume current collection are important as they can lead to performance degradation of the spacecraft systems, enhance erosion and contamination, and cause ESD events. As the spacecraft surfaces collect ions from the thruster plasma plume, those collected by insulating surfaces are neutralized by the plasma electrons, and play no role in generating parasitic currents or determining the spacecraft potential while ions collected by conductive surfaces must be neutralized by electrons collected by the SA tabs and interconnects to achieve current balance, and, therefore, contribute to the generation of parasitic currents. The amount of parasitic currents and level of surface potential are determined by the degree of surface conductivity. Those that are more conductive will provide larger parasitic currents and result in lower surface potentials and vice versa.[18]

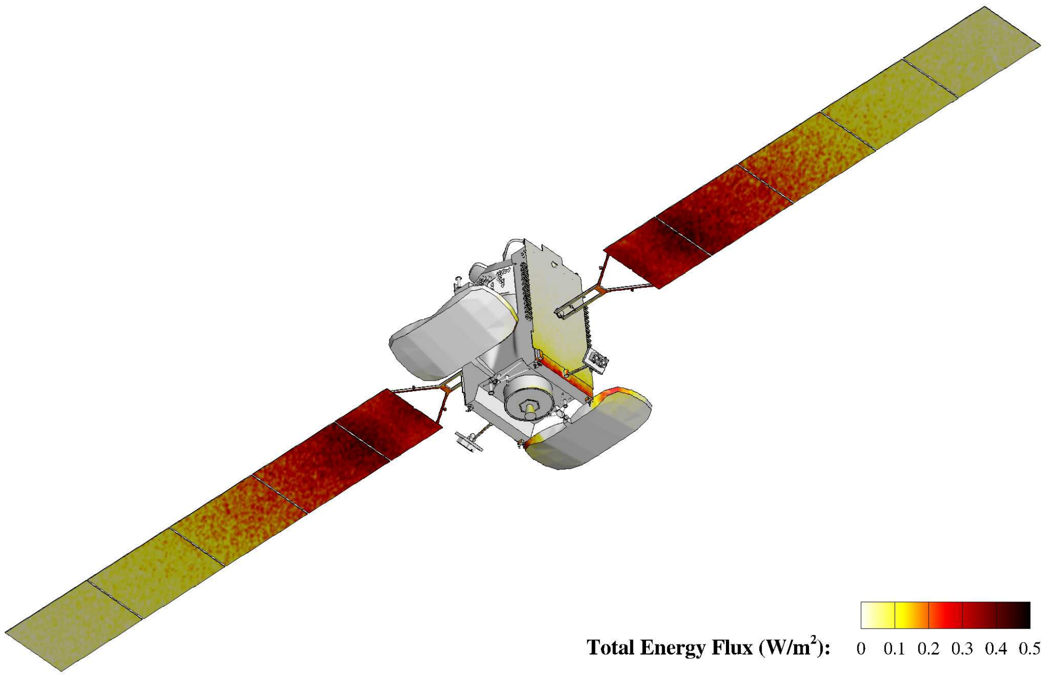

Figure 12. Total energy flux on the spacecraft due to plume impingement from the XR5 HET.

To determine the spacecraft potential, Leidos' NASCAP-2k is used. This computation includes iterations between calculations of the potentials due to the ion density and the charge exchange ion trajectories using those potentials. NASCAP-2k computes the plasma density and currents due to CEX ions using the spacecraft geometry and a plume map of the main beam. The spacecraft geometry discretization and plume map generation are imported from COLISEUM using a combination of Python scripts and third party software that circumvent the need for the PlumeTool and ObjectToolkit modules and helps to streamline the entire numerical analysis process of the plasma plume interaction effects. A surface grid coarsening step as shown in Fig. 13 is required before executing NASCAP-2k.

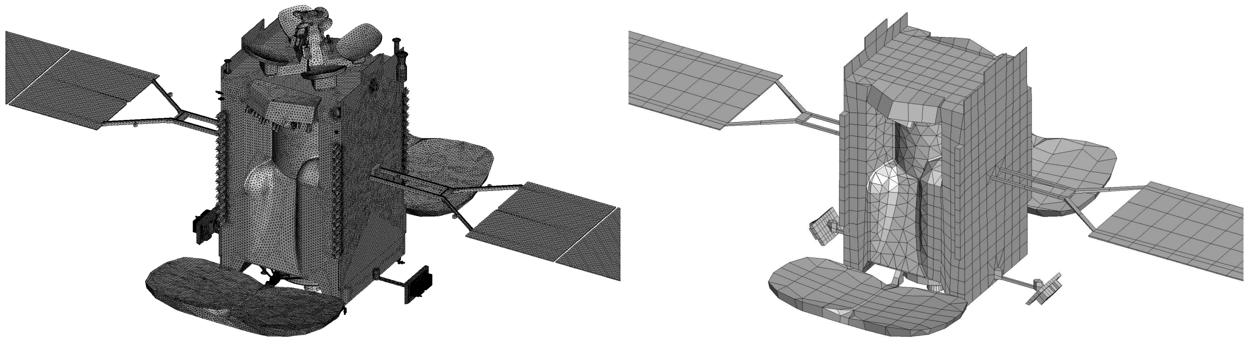

Figure 13. Coarsening process from the COLISEUM surface grid to the NASCAP-2k surface grid.

The floating potential and parasitic currents are established by current balance between the ions incident on conductive surfaces of the spacecraft and electrons collected by biased interconnects and termination tabs on the SA cells using a grounding diagram of the spacecraft and thruster. Surface potentials computed by NASCAP-2k with plume maps imported from COLISEUM are depicted in Fig. 14.

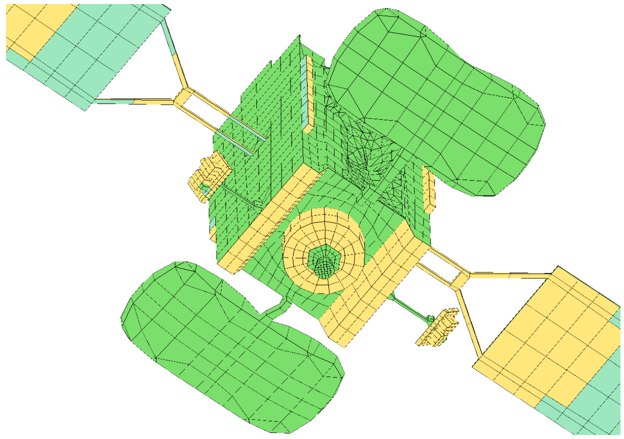

Figure 14. GEOStar surface potentials.

II.D. Electromagnetic Effects

Finally, the effect of the plasma plume on the satellite communications must be also addressed. Noticeable antenna pattern changes can occur for communication signal frequencies within two orders of magnitude of the plasma frequency depending on the antenna geometry and thruster placement. Orbital ATK is currently working towards the adoption of the University of Texas' BeamServer II code to examine and quantify those effects. This code implements a combination of geometrical optics ray tracing and aperture field integration to analyze the effects of plasma thrusters on antenna performance including pointing error (beam squinting), attenuation, sidelobe degradation, and induced cross-polarization.[19] This approach, like the one previously described for the electrical effects, also relies on the plume generated in COLISEUM using HPHall as the particle injection model while allowing the analysis of realistic three-dimensional geometries in a time efficient manner via to the use of a ray tracing code.

In addition to the RF plasma plume propagation effects, the HET also produces strong radiated emissions at frequencies that overlap with commonly used communications frequency bands. The effect of these emissions could be saturation of sensitive receiver amplifiers or increased bit error rates depending again on thruster placement and antenna geometry. This interaction is not covered by the tools described in this paper (i.e. BeamServer II) but addressed through a separate set of tools developed at Orbital ATK.

III. Conclusions and Future Work

Over the last four years Orbital ATK has invested substantial resources in establishing a comprehensive software tool suite that enables reliable M&S of the various interactions between the plasma plume of ion thrusters and the different spacecraft systems. The toolset is based on AFRL's COLISEUM software suite, Leidos' NASCAP-2k, and University of Texas' BeamServer II and augmented with new models and post-processing techniques. It has also been validated with data obtained from a detailed erosion and contamination test campaign and compared against an end-to-end test to understand the potential sources of error and establish the validity of the modeling process. In terms of thruster plumes, the tool now includes the capability to model multiple electric thrusters, namely the XR-5 HET, the NEXT gridded ion thruster, and the TILE electrospray thruster. At this point in time the tool suite has reached sufficient maturity to be deployed on the GEOStar product line, the MEV, and other spacecrafts for national security and human space missions.

While much has been accomplished over this period of time, further development of this toolbox is foreseen. In particular, plans are in place to directly integrate the BeamServer II code into the COLISEUM framework so that the spacecraft payload/antenna engineer is able to study in detail the effects produced by the propagation of the RF signal through the plasma plume. This capability is of particular interest for missions that employ payloads in the lower frequency bands. There are also plans to replace NASCAP-2k with COLISEUM for the evaluation of electrical effects to further simplify the analysis process. Lastly, Orbital ATK intends to further expand the plume effects database to include new spacecraft surface materials and to address other effects that may become important for future spacecraft designs, such as charge dissipative characteristics of certain thin films and RF gain/loss through deposition layers. In conclusion, with the continuing expansion of spacecraft systems that employ electric propulsion, Orbital ATK intends to maintain and continuously improve the M&S tools that are needed by the systems engineers to design spacecraft systems compatible with the plasma plume environment produced by these systems.

Acknowledgments

The authors would like to thank Dr. Justin W. Koo at AFRL/RQRS, Dr. Michelle K. Scharfe at ERC, Inc. and Dr. Lubos Brieda at Particle in Cell Consulting, LLC, for their assistance with the familiarization and usage of COLISEUM and HPHall codes, Dr. Brandon D. Smith and Prof. Iain D. Boyd of University of Michigan for making available their research work and facilitating in that manner the implementation of Xe triple charged ions and the BN erosion effects into the Orbital ATK version of HPHall, and Prof. Gary A. Hallock and Prof. James C. Wiley of University of Texas at Austin for their insights with the usage and capabilities of the BeamServer II code.

References

[1]Yamamura, Y., Itikawa, Y., and Itoh, N., "Angular Dependence of Sputtering Yields of Monatomic Solids," IPPJ-AM-26, Institute of Plasma Physics, Nagoya University, June 1983.

[2]Yamamura, Y. and Tawara, H., "Energy Dependence of Ion-Induced Sputtering Yields from Monatomic Solids at Normal Incidence," *Atomic Data and Nuclear Data Tables*, Vol. 62, No. 2, March 1996, pp. 149–253.

[3]Roussel, J.-F., Bernard, J., and Garnier, Y., "Numerical Simulation of Induced Environment, Sputtering and Contamination of Satellite due to Electric Propulsion," ESA SP-398, August 1997.

[4]Zhang, J., Bhattacharjee, S., Shuttanandan, V., and Ray, P. K., "Sputtering Investigation of Boron Nitride with Secondary Ion and Secondary Neutral Mass Spectrometry," *Journal of Vacuum Science & Technology A: Vacuum, Surfaces, and Films*, Vol. 15, No. 2, March 1997, pp. 243–247.

[5]Smith, B. D., *A Numerical Study of Wall Erosion and Material Transport in Hall Thrusters*, Ph.D. thesis, The University of Michigan, 2015.

[6]Fife, J. M., Gibbons, M. R., VanGilder, D. B., and Kirtley, D. E., "Initial Use of a 3-D Plasma Simulation System for Predicting Surface Sputtering and Contamination by Hall Thrusters," AIAA Paper 2002-2125, *33rd Plasmadynamics and Lasers Conference*, Maui, HI, May 2002.

[7]Noushkam, N., Basak, D., Glogowski, M. J., Crofton, M. W., Young, J. A., and Plecque, B., "Sputtering Effects of Xenon Ion Thruster Plume on Common Spacecraft Materials," AIAA Paper 2015-4642, *AIAA SPACE 2015 Conference and Exposition*, Pasadena, CA, August-September 2015.

[8]Bermúdez, L. M., Noushkam, N., Basak, D., and Glogowski, M. J., "High Fidelity Numerical Simulations for the Characterization of Plasma Plume Interaction Effects on Geostationary Satellites," AIAA Paper 2015-4641, *AIAA SPACE 2015 Conference and Exposition*, Pasadena, CA, August-September 2015.

[9]Hofer, R. R., Mikellides, I. G., Katz, I., and Goebel, D. M., "BPT-4000 Hall Thruster Discharge Chamber Erosion Model Comparison with Qualification Life Test Data," IEPC Paper 2007-267, *30th International Electric Propulsion Conference*, Florence, Italy, September 2007.

[10]Fife, J. M., *Hybrid-PIC Modeling and Electrostatic Probe Survey of Hall Thrusters*, Ph.D. thesis, Massachusetts Institute of Technology, September 1998.

[11]Parra, F. I., Ahedo, E., Fife, J. M., and Martínez-Sánchez, J. M., "A Two-Dimensional Hybrid Model of the Hall Thruster Discharge," *Journal of Applied Physics*, Vol. 100, No. 023304, 2006.

[12]Hofer, R. R., Katz, I., Mikellides, I. G., Goebel, D. M., Jameson, K. K., Sullivan, R. M., and Johnson, L. K., "Efficacy of Electron Mobility Models in Hybrid-PIC Hall Thruster Simulations," AIAA Paper 2008-4924, *44th AIAA/ASME/SAE/ASEE Joint Propulsion Conference & Exhibit*, Hartford, CT, July 2008.

[13]Brieda, L. and Wang, J., "Modeling of Ion Thruster Beam Neutralization Using a Fully Kinetic ES-PIC Code," AIAA Paper 2005-4045, *41st AIAA/ASME/SAE/ASEE Joint Propulsion Conference & Exhibit*, Tucson, AZ, July 2005.

[14]Crofton, M. W., Nocerino, J. C., Young, J. A., and Patterson, M. J., "NEXT Ion Engine Plume Deposition Rates: QCM Measurements," AIAA Paper 2014-0140, *52nd Aerospace Sciences Meeting*, AIAA SciTech Forum, National Harbor, MD, January 2014.

[15]Lozano, P. and Martínez-Sánchez, M., *Studies on the Ion-Droplet Mixed Regime in Colloid Thrusters*, Ph.D. thesis, Massachusetts Institute of Technology, 2003.

[16]Gamero-Castaño, M., "The Structure of Electrospray Beams in Vacuum," *Journal of Fluid Mechanics*, Vol. 604, 2008, pp. 339–368.

[17]Romero-Sanz, I., Bocanegra, R., Fernández De La Mora, J., and Gamero-Castaño, M., "Source of Heavy Molecular Ions Based on Taylor Cones of Ionic Liquids Operating in the Pure Ion Evaporation Regime," *Journal of Applied Physics*, Vol. 94, No. 5, 2003, pp. 3599–3605.

[18]Davis, V. A., Gardner, B. M., and Mandell, M. J., "GEOStar-3 EP IRAD Program Support," Final Report, Leidos, January 2015.

[19]Hallock, G. A., Wiley, J. C., Khanna, A., and Spencer, E. A., "Impact Analysis of Hall Thrusters on Satellite Antenna Performance," *Journal of Spacecraft and Rockets*, Vol. 39, No. 1, January-February 2002, pp. 115–124.